Clim Dyn (2011) 36:1037–1054
DOI 10.1007/s00382-010-0741-2

Sensitivity of simulated terrestrial carbon assimilation and canopy transpiration to different stomatal conductance and carbon assimilation schemes

Haishan Chen · Robert E. Dickinson · Yongjiu Dai · Liming Zhou

Received: 18 July 2009 / Accepted: 5 January 2010 / Published online: 29 January 2010

Abstract Accurate simulations of terrestrial carbon assimilation and canopy transpiration are needed for both climate modeling and vegetation dynamics. Coupled stomatal conductance and carbon assimilation ($A - g_s$) models have been widely used as part of land surface parameterizations in climate models to describe the biogeophysical and biogeochemical roles of terrestrial vegetation. Differences in various $A - g_s$ schemes produce substantial differences in the estimation of carbon assimilation and canopy transpiration, as well as in other land–atmosphere fluxes. The terrestrial carbon assimilation and canopy transpiration simulated by two different representative $A - g_s$ schemes, a simple A–g_s scheme adopted from the treatments of the NCAR model (Scheme I) and a two-big-leaf $A - g_s$ scheme newly developed by Dai et al. (J Clim 17:2281–2299, 2004) (Scheme II), are compared via some sensitivity experiments to investigate impacts of different $A - g_s$ schemes on the simulations. Major differences are found in the estimate of canopy carbon assimilation rate, canopy conductance and canopy transpiration between the two schemes, primarily due to differences in (a) functional forms used to estimate parameters for carbon assimilation sub-models, (b) co-limitation methods used to estimate carbon assimilation rate from the three limiting rates, and (c) leaf-to-canopy scaling schemes. On the whole, the differences in the scaling approach are the largest contributor to the simulation discrepancies, but the different methods of co-limitation of assimilation rate also impact the results. Except for a few biomes, the residual effects caused by the different parameter estimations in assimilation sub-models are relatively small. It is also noted that the two-leaf temperature scheme produces distinctly different sunlit and shaded leaf temperatures but has negligible impacts on the simulation of the carbon assimilation.

H. Chen (✉)
Key Laboratory of Meteorological Disaster of Ministry of Education, Nanjing University of Information Science & Technology, 210044 Nanjing, China
e-mail: haishan@nuist.edu.cn

H. Chen · R. E. Dickinson · L. Zhou
School of Earth and Atmospheric Sciences, Georgia Institute of Technology, Atlanta, GA 30332-0340, USA

Present Address:
R. E. Dickinson
Department of Geological Sciences, The University of Texas at Austin, Austin, TX 78712, USA

Y. Dai
State Key Laboratory of Earth Surface Processes and Resource Ecology, School of Global Change and Earth System Science, Beijing Normal University, 100875 Beijing, China

1 Introduction

Vegetation plays an important role in climate change, and land–atmosphere exchanges are in part controlled over vegetated regions through the stomatal resistance of leaves. In earlier land surface models, such as BATS (Dickinson et al. 1986, 1993) and SiB (Sellers et al. 1986), empirical models of the stomatal resistance based on Jarvis (1976) were widely used to describe the biophysical control of evapotranspiration and to provide more realistic estimation of the land–atmosphere fluxes. With increasingly scientific interest in global climate change, the need for more complete models of the climate system including biological and chemical processes has become apparent. Since the carbon flux exchange between terrestrial ecosystems and the atmosphere is one of most important components of the global carbon cycle, the parameterizations that provide

realistic and accurate estimation of CO_2 flux through vegetation are needed for both climate modeling and ecosystem modeling. Biochemical models of carbon assimilation have been extensively incorporated into climate models to describe the biogeochemical roles of the terrestrial vegetation, and in particular coupled stomatal conductance and carbon assimilation ($A - g_s$) models have been widely used in the third generation land models (Sellers et al. 1996; Bonan 1996; Dickinson et al. 1998) to describe stomatal control of vegetation transpiration as well as the exchange of carbon between the vegetated land surface and the atmosphere (Sellers et al. 1997).

Farquhar et al. (1980) developed a widely used carbon assimilation model which has been modified by many researchers (Collatz et al. 1990, 1991; Harley et al. 1992; Harley and Baldocchi 1995; Leuning 1995) and has been extended to couple the stomatal conductance to the carbon assimilation (Ball et al. 1987, 1988; Leuning 1990; Collatz et al. 1991). The carbon assimilation model for C4 plants basically comes from that of Collatz et al. (1992). Such models have been developed at the leaf level, and must be scaled to the canopy level for coupling to the atmosphere (Baldocchi and Harley 1995; Leuning et al. 1995; Kull and Kruijt 1998; Kull and Jarvis 1995; Walcroft et al. 1997; Dang et al. 1997).

The methods used for leaf to canopy scaling can be divided into three categories, i.e., one-big-leaf models, two-big-leaf (sunlit/shaded) models, and multi-layer models. Multilayer models can use parameters measured at the leaf level, in which the canopy photosynthetic rate is computed by integrating the environmental and physiological variables within the canopy. They can be calibrated from leaf-level measurements as long as the spatial pattern of parameters and physiological factors are represented (Wang and Jarvis 1990; Jarvis 1993, 1995; Leuning et al. 1995; Baldocchi and Harley 1995; Larocque 2002). Due to their complexity, multi-layer models are not widely used in climate models or global carbon cycle models. On the contrast, the big-leaf models have been extensively used in land surface climate modeling because they require fewer parameters and are computationally efficient (Sellers et al. 1996; Bonan 1996; Dickinson et al. 1998; Dai et al. 2003). The one-big-leaf models assume that the integrated characteristics of the whole canopy can be represented as a single, horizontally extended big leaf for the computation of canopy carbon assimilation rate and other fluxes (Sellers et al. 1992, 1996). However, carbon assimilation is determined by photosynthetically active radiation (PAR) and temperatures that differ between sunlit and shaded leaves (Sinclair et al. 1976; Norman 1993). Thus, the one-big-leaf models could significantly overestimate the canopy carbon assimilation rate by neglecting these differences (Spitters 1986; Wang and Leuning 1998). The two-big-leaf (sunlit/shaded) models, which stratify a canopy into sunlit and shaded portions, have been introduced into land surface models (Bonan 1996; de Pury and Farquhar 1997; Dickinson et al. 1998; Wang and Leuning 1998; Dai et al. 2004). The models of Bonan (1996) and Dickinson et al. (1998) treat the carbon assimilation and stomatal conductance of sunlit leaves separately from those of shaded leaves but use a single leaf temperature, while the two-big-leaf models developed by Wang and Leuning (1998) and Dai et al. (2004) calculate separately leaf temperatures and fluxes for the sunlit and shaded canopy.

The stomatal conductance and carbon assimilation ($A - g_s$) parameterizations used in land surface simulations have been continuously improved by incorporating the knowledge acquired from plant physiological research. However, with increasing complexity model details diverge in various aspects, such as in their scaling schemes, photosynthetic parameter estimations and computational schemes as well as other relevant treatments.

To provide an example of the consequences of such differences, two different $A - g_s$ parameterization schemes are compared to evaluate the impacts of different treatments of stomatal conductance and carbon assimilation on the simulation of carbon assimilation rate and canopy transpiration in this study. The two $A - g_s$ schemes are briefly described in Sect. 2 and designs of sensitivity experiments are given in Sect. 3. Results and further explanations with respect to reasons for the differences are discussed in Sect. 4, followed by a summary in Sect. 5.

2 Description of stomatal conductance and carbon assimilation schemes

2.1 Relatively simple $A - g_s$ parameterization scheme (Scheme I)

Scheme I is a relatively simple $A - g_s$ parameterization for the stomatal conductance and carbon assimilation, which was used in the early NCAR Land Surface Model (NCAR LSM1.0, Bonan 1996). The new NCAR Community Land Model (CLM3.0, Oleson et al. 2004) has a different treatment of leaf light levels than the earlier one used by Bonan (1996), whose impact is not addressed here, but otherwise uses the same scheme. The leaf carbon assimilation rate is estimated by using a leaf carbon assimilation biochemical model, and the leaf stomatal resistance is coupled to the leaf carbon assimilation rate (Eq. in Table 1). The basic equations and relevant parameters for Scheme I are summarized in Tables 1 and 2.

The carbon assimilation rate is estimated as the minimum of three assimilation limited rates (Eq. 2b). Three limiting rates, i.e., the Rubisco limited rate w_c, the light-limited rate w_j and the carbon compound export limitation (C3 plants) or

Table 1 Comparison of two $A - g_s$ schemes

Process	Scheme	
	Scheme II	Scheme I
A. Carbon assimilation sub-model:		
1. Three limiting rates of assimilation		
(1) Rubisco limited rate:	$w_c = \begin{cases} \frac{(c_i - \Gamma_*)V_m}{c_i + K_c(1 + o_i/K_o)} & \text{for } C_3 \\ V_m & \text{for } C_4 \end{cases}$ (1)	Same
CO_2 compensation point:	$\Gamma_* = 0.5 \times o_i/(2,600 \times 0.57^{Q_{10}})$ (2a)	$\Gamma_* = 0.5(K_c/K_o) \times 0.21 \times o_i \approx 0.5 \times o_i/(4,762 \times 0.57^{Q_{10}})$ (2b)
Maximum catalytic capability of Rubisco:	$V_m = V_{\max} f_T(T_l) f_w(\theta)$ (3)	Same
Leaf temperature dependence of V_m:	$f_T(T_l) = \begin{cases} \frac{2.1^{Q^{10}}}{\{1 + e^{0.3(T_l - s_2)}\}} & \text{for } C_3 \\ \frac{2.1^{Q^{10}}}{\{1 + e^{0.3(T_l - s_2)}\}/\{1 + e^{0.2(s_4 - T_l)}\}} & \text{for } C_4 \end{cases}$ (4a)	$f_T(T_l) = \frac{2.4^{Q^{10}}}{[1+e^{(710T_l - 220000)/RT_l}]}$ (4b)
Soil water limited factor:	$f_w(\theta) = \sum_{i=1}^{nsoil} \{r_i[(\psi_{\max} - \psi_i)/(\psi_{\max} + \psi_{sat,i})]\}$ (5)	Same
(2) Light-limited rate:	$w_j = \begin{cases} \frac{J(c_i - \Gamma_*)}{c_i + 2\Gamma_*} & \text{for } C_3 \\ J & \text{for } C_4 \end{cases}$ (6)	Same
Electron transport rate for given absorbed PAR (ϕ):	$J = \min(\varepsilon\alpha\phi, J_m/4)$ (7a) where $\alpha = 4.6$ μmol J^{-1} is used to covert ϕ (W m^{-2}) to photosynthetic photon flux (μmol m^{-2} s^{-1})	$J = \varepsilon\alpha\phi$ (7b) Same
Potential electron transport rate:	$J_m = J_{\max} f_T(T_l) f_w(\theta)$ (8)	
	$J_{\max} = 2.1 V_{c\max}$ (9)	None
Leaf temperature dependence of J_m:	$f_T(T_l) = \frac{e^{(10Q^{10}E_a)/(298RT_l)}[1+e^{(298S-H)/(298R)}]}{[1+e^{(ST_l-H)/RT_l}]}$ (10)	
(3) Carbon compound export limitation (C3 plants) or PEP-carboxylase limitation (C4 plants)	$w_e = \begin{cases} 0.5V_m & \text{for } C_3 \\ 2 \times 10^4 V_m \frac{c_i}{P_{atm}} & \text{for } C_4 \end{cases}$ (11a)	$w_e = \begin{cases} 0.5V_m & \text{for } C_3 \\ 4,000 V_m \frac{c_i}{P_{atm}} & \text{for } C_4 \end{cases}$ (11b)
2. Estimation of assimilation rate A		
Assimilation rate are described by combining three limiting rates into two quadratic equations, which are then solved for their smaller roots:	$\beta_{cj} w_p^2 - w_p(w_c + w_j) + w_c w_j = 0$ $\beta_{pe} A^2 - A(w_p + w_e) + w_p w_e = 0$ (12a) Where w_p is a temporary variable, $\beta_{cj} = 0.877$ and $\beta_{pe} = 0.99$ are canopy photosynthesis curvature factors	Assimilation rate is assume to be the minimum of the three limiting rates: $A = \min(w_c, w_j, w_e)$ (12b)

Table 1 continued

Process	Scheme	
	Scheme II	Scheme I
	Net assimilation (mol m^{-2} s^{-1}): $A_n = A - R_d$ (13)	No respiration rate calculated
	Dark respiration rate: $R_d = f_d V_m$ (14)	
	Leaf temperature dependence of V_m used here is: $f_T(T_l) = \frac{2.1^{Q^{10}}}{\{1+e^{1.3(T_l-328.16)}\}}$ (15)	
3. Leaf to canopy scaling scheme		
	Leaf to canopy vertical integration scheme	Average scheme
	Rubisco capacity $V_{\max}$:	$V_{\max} = V_{c\max}$ (16b)
	$V_{\max} = V_{c\max}\exp(-k_n x)$ (16a)	
	Photosynthetic capacity of sunlit and shaded canopy:	
	$[V_{\max}]_{\text{sun}} = \int_0^{L_{AI}} V_{\max}(x) f_{\text{sun}}(x)dx = C_{1\text{sun}} \times V_{c\max}$ (17a)	$V_{\max} = V_{c\max}$ (17b)
	$[V_{\max}]_{\text{sha}} = \int_0^{L_{AI}} V_{\max}(x) f_{\text{sha}}(x)dx = C_{1\text{sha}} \times V_{c\max}$ (18a)	$V_{\max} = V_{c\max}$ (18b)
	Scaling factors used are:	
	$C_{1\text{sun}} = [1 - e^{-(k_n+k_b)L_{AI}}]/(k_n + k_b)$ (19)	
	$C_{1\text{sha}} = [1 - e^{-k_n L_{AI}}]/k_n - [1 - e^{-(k_n+k_b)L_{AI}}]/(k_n + k_b)$ (20)	
	Potential electron transport:	
	$J_{\max} = J_{c\max}\exp(-k_d x)$ (21)	None
	Potential electron transport for sunlit/shaded canopy:	
	$[J_{\max}]_{\text{sun}} = \int_0^{L_{AI}} J_{\max}(x) f_{\text{sun}}(x)dx = C_{2\text{sun}} \times J_{c\max}$ (22)	None
	$[J_{\max}]_{\text{sha}} = \int_0^{L_{AI}} J_{\max}(x) f_{\text{sha}}(x)dx = C_{2\text{sha}} \times J_{c\max}$ (23)	
	Scaling factors are given by:	
	$C_{2\text{sun}} = (1 - e^{-(k_d+k_b)L_{AI}})/(k_d + k_b)$ (24)	
	$C_{2\text{sha}} = (1 - e^{-k_d L_{AI}})/k_d - \{[1 - e^{-(k_d+k_b)L_{AI}}]/(k_d + k_b)\}$ (25)	
B. Stomatal conductance model		
	$g_s = m\frac{A_n e_s}{c_s e_i}P_{\text{atm}} + b$ (26a)	$\frac{1}{r_s} = m\frac{A e_s}{c_s e_i}P_{\text{atm}} + b$ (26b)
	Scaling to canopy:	
	$[g_s]_{\text{sun}} = m\left[\frac{A_n e_s}{c_s e_i}\right]_{\text{sun}} P_{\text{atm}} + b f_w(\theta) \times C_{3\text{sun}}$ (27)	
	$[g_s]_{\text{sha}} = m\left[\frac{A_n e_s}{c_s e_i}\right]_{\text{sha}} P_{\text{atm}} + b f_w(\theta) \times C_{3\text{sha}}$ (28)	
	$C_{3\text{sun}} = (1 - e^{-k_b L_{AI}})/k_b = L_{\text{sun}}$ (29)	
	$C_{3\text{sha}} = L_{AI} - (1 - e^{-k_b L_{AI}})/k_b = L_{\text{sha}}$ (30)	

PEP-carboxylase limitation (C4 plants) w_e, are given by Eqs. (1), (6) and (11b), respectively. One of the most important model parameters is the maximum rate of carboxylation V_m, which depends on the physiological parameter $V_{\max}$ of each plant functional type (PFT), and is also adjusted by a leaf temperature dependence function $f_T(T_l)$ and a soil moisture limitation function $f_w(\theta)$ (Eq. 3). The maximum photosynthetic capacity at 25°C, $V_{\max}$, is assumed to be constant at all the canopy levels and is set to the maximum Rubisco capacity at the canopy top per leaf area ($V_{c\max}$) (Eq. 16b). The absorbed PAR together with the vegetation dependent parameter ε, i.e., quantum yield of electron transport, is used to calculate the electron transport rate J (Eq. 7b).

The relatively simple scheme estimates carbon assimilation (A) and stomatal conductance (g_s) for the sunlit and shaded leaves per unit leaf area index (LAI) by using an average of absorption of direct and diffuse PAR, in which a common leaf temperature is calculated and used for both sunlit and shaded leaves. Then the total assimilation rate and canopy stomatal conductance are estimated by multiplying assimilation rates of sunlit leaves and shaded leaves per unit LAI by sunlit LAI (L_{sun}) and shaded LAI (L_{sha}) (Eqs. 29–30).

2.2 CoLM two-big-leaf $A - g_s$ scheme (Scheme II)

The CoLM two-big-leaf $A - g_s$ scheme (Scheme II) is a new and more complex scheme for the calculation of canopy temperature, carbon assimilation and stomatal conductance developed more recently by Dai et al. (2004). Its basic equations and related parameters are summarized in Table 1. It separately calculates sunlit and shaded leaf temperatures. Its leaf to canopy scaling scheme considers the

Table 2 Model parameters and variables of $A - g_s$ schemes

Definition	Symbol	Unit
Maximum Rubisco capacity at top canopy at 25°C per leaf area	V_{cmax}	mol m^{-2} s^{-1}
One-half point of high temperature inhibition function	s_2	K
One-half point of low temperature inhibition function	s_4	K
Quantum yield of electron transport	ε	mol mol^{-1}
Root fraction within soil layer	r_i	–
Rubisco Michaels–Menten constant for CO_2	$K_c = 30 \times 2.1^{Q_{10}}$	Pa
Rubisco inhibition constant for oxygen	$K_o = 30,000 \times 1.2^{Q_{10}}$	Pa
Q_{10} temperature coefficient	$Q_{10} = (T_l - 298.16)/10$	–
Activation energy	$E_a = 37,000$	J mol^{-1}
Electron-transport temperature response parameter	$S = 710$	J mol^{-1}
Curvature parameter for J_{max}	$H = 2.2 \times 10^5$	J mol^{-1} K^{-1}
Universal gas constant	$R = 8.314$	J mol^{-1} K^{-1}
Extinction coefficients for diffuse PAR	$k_d = 0.719$	–
Coefficients of leaf nitrogen allocation within canopy	$k_n = 0.5$	–
Direct beam extinction coefficients of the canopy	k_b	–
Soil water matric potential	ψ_i	mm
Wilting point soil matric potential of leaf	$\psi_{max} = -1.5 \times 10^5$	mm
Saturated soil water matric potential	$\psi_{sat,i}$	mm
Dark respiration of leaf at 20°C	$f_d = 0.015$ for C3 0.025 for C4	–
Stomatal slope factor	m	–
Minimum stomatal conductance	b	mol m^{-2} s^{-1}
Partial pressure of CO_2 in interior leaf, at leaf surface	c_i,c_s	Pa
Partial pressure of CO_2 in canopy air	$c_a = 355 \times 10^{-6} P_{atm}$	Pa
Partial pressure of O_2 in leaf interior	$o_i = 0.209\ P_{atm}$	Pa
Leaf temperature	T_l	K
Electron transport rate	J	mol m^{-2} s^{-1}
Potential electron transport rate	J_m	mol m^{-2} s^{-1}
Leaf stomatal conductance	g_s	mol m^{-2} s^{-1}
Canopy stomatal conductance	$[g_s]$	mol m^{-2} s^{-1}
Atmospheric pressure at surface	P_{atm}	Pa
Partial pressure of H_2O in canopy air, at leaf surface and inside the leaf	e_a, e_s,e_i	Pa

vertical variations of leaf physiological properties within the plant to provide separate leaf assimilation rates and stomatal conductances for both the sunlit and shaded canopy.

The assimilation rate for Scheme II is also estimated from three limiting rates w_c, w_j and w_e, but with some modifications to the estimations of model parameters (Table 1). Different empirical formula was used to estimate Γ_* and $f_T(T_l)$ (Eqs. 2a and 4a), and a co-limitation as given by Eq. (7a) was used to estimate the electron transport rate J. In addition, the assimilation rate is calculated by solving two quadratic equations (Eq. 12a).

The model equations are integrated over the canopy depth to produce the canopy values for sunlit and shaded leaves individually, based on two basic assumptions: (1) the maximum Rubisco capacity V_{max} is related to the leaf nitrogen concentration (Field 1983; Leuning et al. 1991; Harley et al. 1992), and the vertical profile of leaf nitrogen decreases exponentially with cumulative relative leaf area index, x, from the top of the canopy (Hirose and Werger 1987; Leuning et al. 1995; de Pury and Farquhar 1997); (2) the potential electron transport rate, J_{max}, was assumed to decrease exponentially from the top to the bottom, as expressed in Eq. (21) (Wang and Polglase 1995; Wang and Leuning 1998). The V_{max} and J_{max} integrated over the canopy and photosynthetic capacities and potential electron transport rates for the sunlit and shaded canopy are used according to Eqs. (17a–18a) and Eqs. (22–23).

2.3 Differences between the two $A - g_s$ schemes

The main differences between Scheme I and Scheme II as summarized in Table 1 are discussed below:

(1) Different carbon assimilation sub-model parameters are used: a different leaf temperature response function $f_T(T_l)$ is used for V_{max} (Eq. 4a vs. 4b) and different formula are used to estimate CO_2 compensation point Γ_* (Eq. 2a vs. 2b), and only Scheme II restricts the electron transport rate (Eq. 7a vs. 7b).

(2) Different co-limitation methods are used for estimating the assimilation rate: Scheme I assumes that the carbon assimilation rate is the minimum of three limiting rates (referred to as the "minimum" method), but Scheme II calculates the carbon assimilation rate by solving two quadratic equations based on three limiting rates, and hence avoiding an abrupt transition among different limitation rates (referred to as the "smoothing" method) (Eq. 12a vs. 12b).

(3) A different leaf-to-canopy scaling scheme is used: In Scheme I, the assimilation equations are solved for both sunlit and shaded leaves per LAI, and then the averages of conductance and canopy carbon assimilation rate are weighted by the fractions and leaf area indices of the sunlit and shaded leaves (Eqs.16b–18b), which is referred to as the "averaging" scheme. In Scheme II, however, the leaf-to-canopy scaling scheme considers the vertical variations of the leaf physiological properties and diffuse light within the canopy, to aggregate the assimilation rate and stomatal conductance from the leaf to the sunlit and shaded canopy separately (referred to as the "scaling" scheme) (Eqs. 16a–25).

(4) Different leaf temperature calculation schemes are used: Scheme I only calculates and uses one common leaf temperature to estimate the stomatal conductance and assimilation rates for both sunlit and shaded leaves. Scheme II calculates the sunlit and shaded leaf temperature individually and uses them for the calculation of separate stomatal conductance and assimilation rates for the sunlit and shaded canopy.

Differences in methods used for PAR calculations between the two schemes are not examined. Rather, the same PAR scheme is used in both models to focus on evaluating and recognizing the impacts of different treatments in $A - g_s$ schemes. The PAR scheme in CoLM (Dai et al. 2004) is used throughout the study.

3 Design of sensitivity experiments

The land surface model used is the improved version of the Common Land Model, referred to as CoLM so designated to avoid confusion with different versions of NCAR Community Land Model (CLM2.0, Bonan et al. 2002; CLM3.0, Oleson et al. 2004 and Dickinson et al. 2006). The Common Land Model (CLM initial version) was developed by incorporating the best features of three existing land models, i.e., BATs (Dickinson et al. 1993), IAP94 (Dai and Zeng 1997) and NCAR LSM1 (Bonan 1996, 1998), which was documented by Dai et al. (2001) and introduced to the modeling community in Dai et al. (2003). CoLM has been developed on the basis of its initial version with several important improvements, including: (1) a two-big-leaf model for leaf temperatures and carbon assimilation–stomatal resistance (Dai et al. 2004) and (2) an improved two-stream approximation model for the canopy radiation transfer with separate integrations of radiation absorption by sunlit and shaded fractions of canopy (Dai et al. 2004; Dai 2005).

The Global Soil Wetness Project Period 2 (GSWP2) global $1^\circ \times 1^\circ$ near-surface meteorological datasets spanning from July 1982 to December 1995 (Zhao and Dirmeyer 2003) are used to force CoLM. Most of model parameters used including V_{cmax} (cf Table 2), are the same as those documented by Oleson et al. (2004). Parameters used only in Scheme II are taken from the default values of CoLM. Some functional differences are maintained (cf Eq. 2 and Eq. 4 in Table 1). The boundary condition datasets used are provided by the standard datasets of NCAR CLM3.0, except for a new LAI dataset developed by Tian et al. (2004a, b) based on MODIS products.

Three experiments of 13.5-year global simulations were performed by using the CoLM with different $A - g_s$ schemes, i.e., Scheme I (Exp. CoLM_I), Scheme II (Exp. CoLM_II), and a modification of Scheme II with only one common leaf temperature calculated (Exp. CoLM_II_2L1T). All experiments were integrated from July 1983 to December 1995. The average of the last 10 years of the results was investigated. Comparisons of model results between Exp. CoLM_I and CoLM_II explore the differences produced by the two different $A - g_s$ schemes, while the comparisons between Exp. CoLM_II and CoLM_II_2L1T examine the impacts resulting from the differences in leaf temperature computation schemes.

Three additional experiments, i.e., Exp. CoLM_II_sm, Exp. CoLM_II_scale and Exp. CoLM_II_sm_scale, were also carried out to quantitatively evaluate the impacts of different treatments used in the carbon assimilation models. Table 3 summarizes these runs. Exp. CoLM_II_sm is the same as Exp. CoLM_II except for replacing the solution of the quadratic equations used in Scheme II with the minimum value method of Scheme I, Exp. CoLM_II_scale replaces the original scaling scheme of Scheme II by the average scheme used in Scheme I; Exp. CoLM_II_sm_scale removes both the smoothing of quadratic equations and the original scaling method of Scheme II.

Table 3 Brief description of different sensitivity runs

Experiments	Description
CoLM_I	Scheme I: same sun and shade leaf temperature, same V_{max}, no co-limitation used
CoLM_II	Scheme II: different sun and shade leaves temps, variable V_{max}, co-limitation used
CoLM_II_2L1T	Scheme II: with one common leaf temperature
CoLM_II_scale	Scheme II: no variable V_{max}, i.e., the original scaling method is removed from Scheme II
CoLM_II_sm	Scheme II: no co-limitation, i.e., the smoothing of quadratic equations is removed from Scheme II
CoLM_II_sm_scale	Scheme II: no co-limitation, no variable V_{max}, i.e., both the smoothing of quadratic equations and the original scaling method are removed from Scheme II

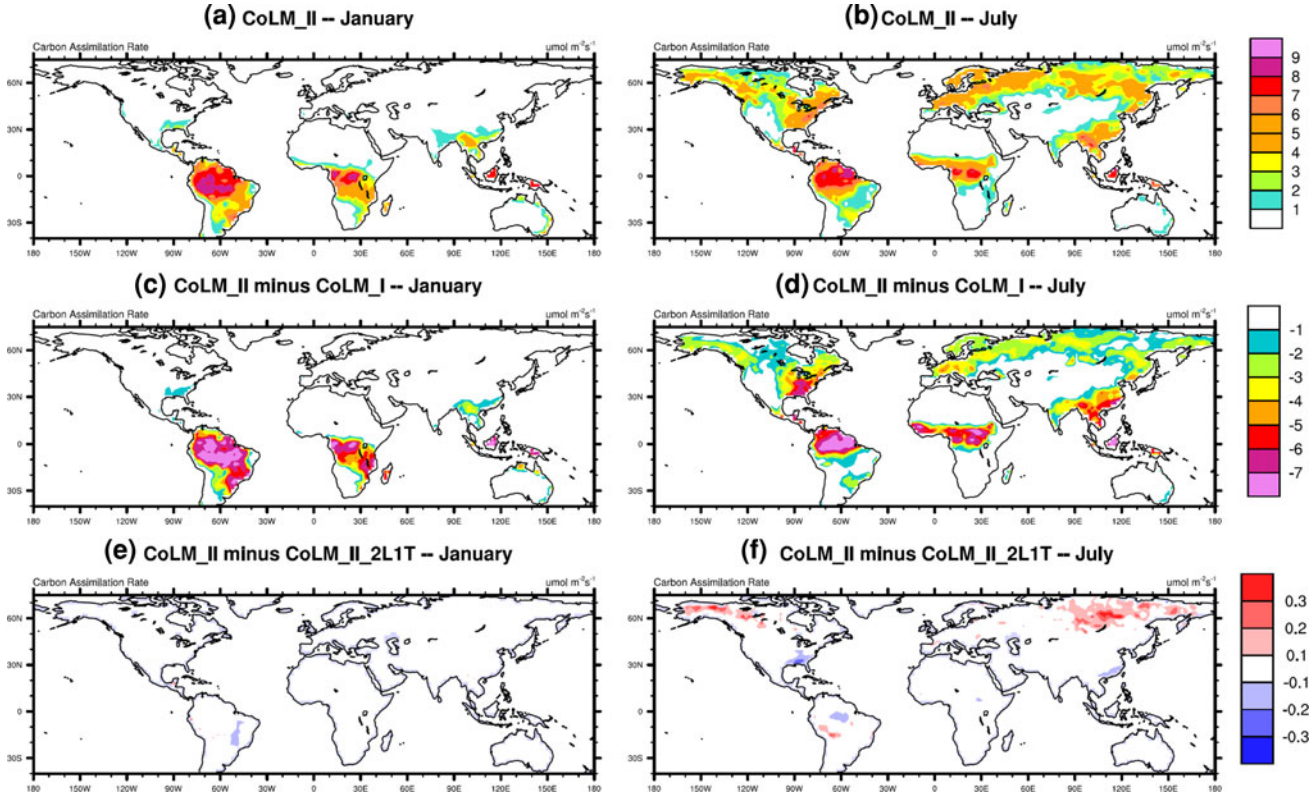

Fig. 1 Carbon assimilation rates simulated by different $A - g_s$ schemes: January (**a**) and July (**b**) monthly average from Exp. CoLM_II; January (**c**) and July (**d**) difference (Exp. CoLM_II minus Exp. CoLM_I); January (**e**) and July (**f**) difference (Exp. CoLM_II minus Exp. CoLM_II_2L1T)

4 Results and discussion

4.1 Impacts of overall differences between parameterizations

Figure 1 presents the global distribution of monthly carbon assimilation rates simulated by CoLM with the two $A - g_s$ schemes in January and July. It shows that Scheme I produces much larger assimilation rates in both seasons (Fig. 1c, d) than Scheme II. The assimilation rates in Scheme I are nearly twice as large as those in Scheme II in the Tropics and about 70–80% larger in the mid- and high- latitudes of the North American and Eurasian Continents (Fig. 1a, b). The large differences in the tropics are mainly related to the strong photosynthetic activity of the tropical vegetation. As a result, both the canopy conductance (Fig. 2a, b) and the canopy transpiration (Fig. 2e–f) are also significantly larger in CoLM_I. The canopy conductance was larger by 3–5 mm/s in both January and July over most tropical regions, but only by $\sim$1 mm/s in July in the northern temperate and boreal regions. Similar increases by up to 20–30 Wm^{-2} were found in the simulated canopy transpiration in the Tropics. The differences of the simulated canopy transpiration have a similar but not

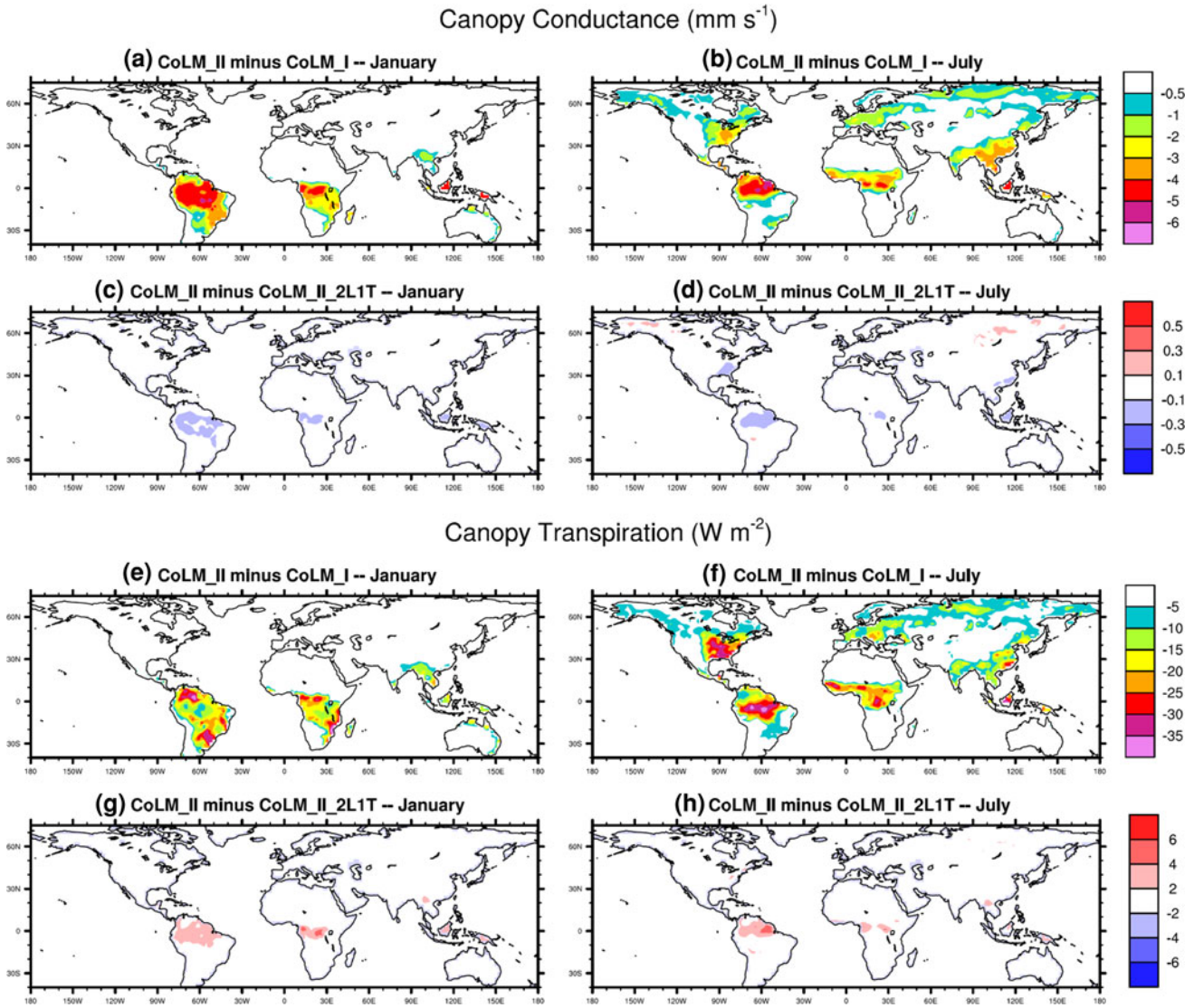

Fig. 2 Differences in simulated canopy conductance (**a**–**d**) and canopy transpiration (**e**–**h**)

identical pattern as those of the assimilation rates, possibly due to spatial differences in the relevant atmospheric environmental variables.

The seasonal cycles of the simulated assimilation rates and relevant variables averaged over each of six selected regions are further investigated. The assimilation rates estimated by CoLM_I are evidently much higher than those by CoLM_II in almost all months over all regions. The differences are largest in the two tropical regions, smallest in the two northern boreal regions, and in-between in the two sub-tropical regions (Fig. 3). The regionally averaged canopy conductance and assimilation rate (Fig. 4) exhibit similar seasonal cycles, with Scheme I giving a relatively larger canopy conductance than Scheme II. Scheme I also gives higher values in simulated canopy transpiration (Fig. 5). The canopy transpiration in the Amazon and Congo Basins is larger in the dry season but the canopy conductance is larger in the wet season. This seasonal discrepancy is caused by the seasonality of climate factors in those regions. Canopy transpiration is also proportional to the gradient of humidity between leaf and air, and so can increase with decreased canopy conductance if this gradient is large enough. Because the gradient of humidity between leaf and air is 3–4 times larger in the dry than in the wet season, this factor overcomes the decrease of canopy conductance.

Further comparisons between Scheme I and Scheme II were also performed on the basis of different PFTs. The first two panels of Fig. 6 show the simulated differences in carbon assimilation rates for each PFT in January and July, normalized by the CoLM_II results. In January, the assimilation rate in Scheme I is larger by more than

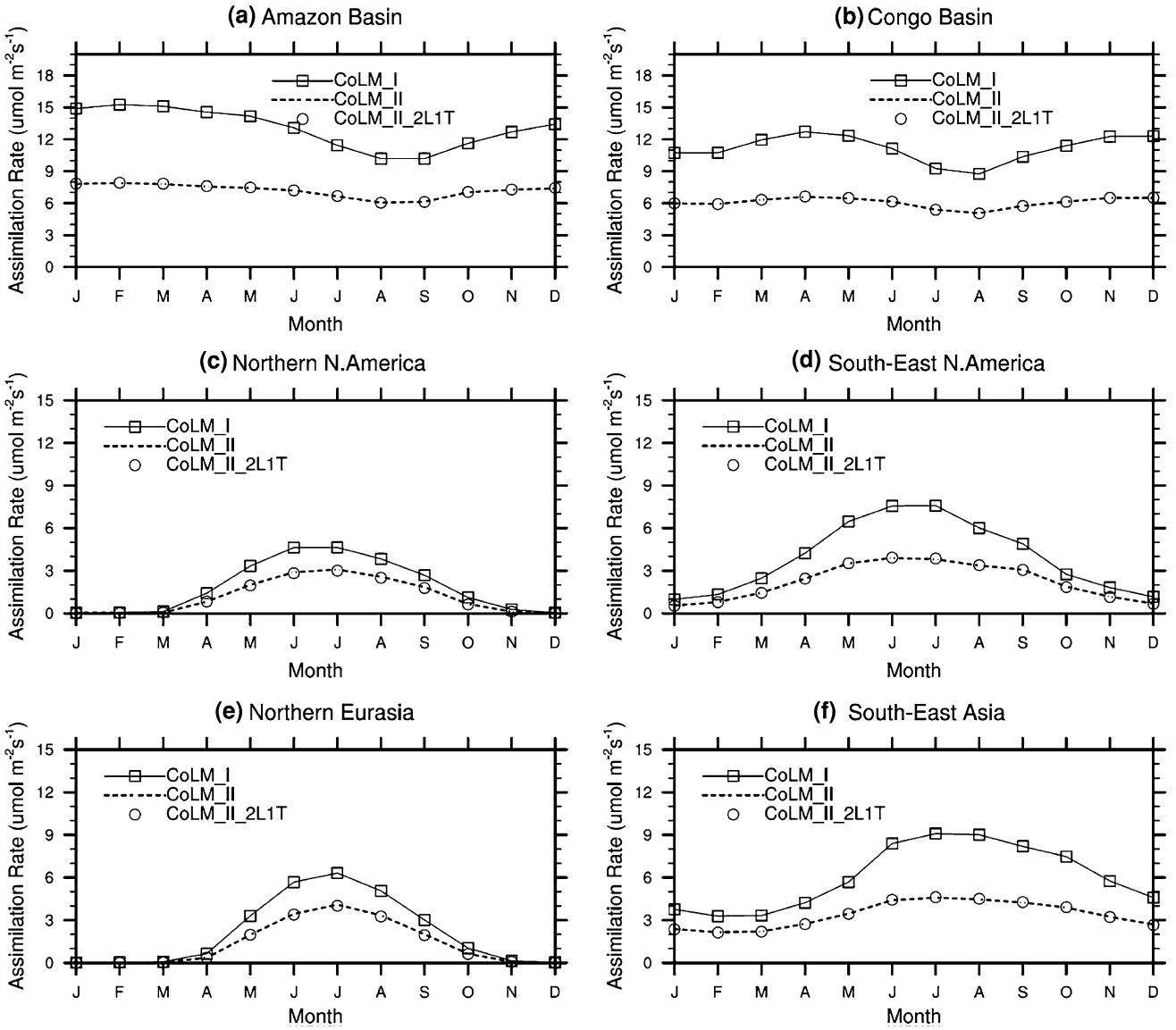

Fig. 3 Monthly carbon assimilation rate simulated by Exp. CoLM_I (*square*), CoLM_II (*dotted line*) and CoLM_II_2L1T (*circle*) averaged over six selected regions. The six regions are Amazon Basin (0–10°S, 50°–70°W), Congo Basin (5°S–5°N, 10°–30°E), Northern North America (50°–70°N, 90°–120°W), South–East North America (30°–50°N, 80°–100°W), Northern Eurasian Continent (50°–70°N, 10°–140°E), and South–East Asia (10°–30°N, 90°–120°E)

60–75% for most PFTs, and even over 100% for C3 grass, C4 grass and crop1 (Fig. 6a). Lower values of about 40% are seen for boreal broadleaf deciduous tree (BDT-Boreal) and temperate broadleaf evergreen shrub (BES-temperate) in July (Fig. 6b). This comparison is less meaningful when the assimilation rates are very small, such as those of NET Boreal, BDT Boreal and BDS Boreal PFTs in January.

4.2 Sunlit/shaded temperature effects

As discussed in Sect. 2, only one common leaf temperature was calculated and used in the calculations of carbon assimilation rates for both sunlit and shaded leaves in Scheme I. Scheme II calculates and uses separate sunlit and shaded leaf temperatures for the calculation of assimilation rates of the sunlit and shaded canopy. Earlier research has shown that such a treatment could contribute to differences in simulated carbon assimilation rates between one-big-leaf and two-big-leaf models (Wang and Leuning 1998; Dai et al. 2004). In particular, Wang and Leuning (1998) pointed out that sunlit leaves can be several degrees warmer than shaded leaves under sunny and dry conditions, and ignoring this temperature difference will bias the estimates of the carbon assimilation rate, sensible and latent heat. However, they did not quantify such differences.

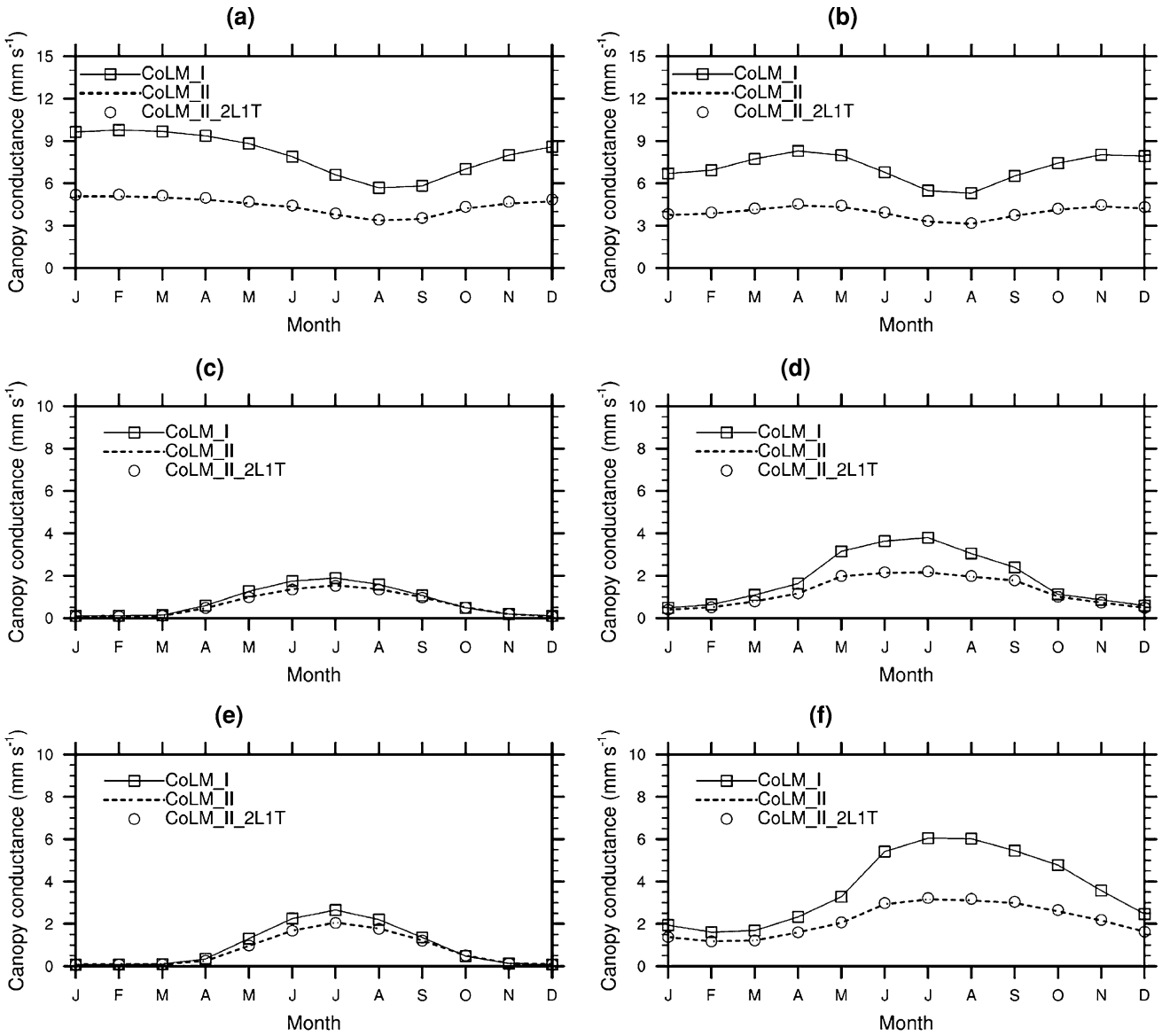

Fig. 4 As in Fig. 3, but for canopy conductance. **a** Amazon Basin, **b** Congo Basin, **c** Northern North America, **d** South–East North America, **e** Northern Eurasian, **f** South–East Asia

Results simulated by CoLM_II_2L1T and CoLM_II are compared to investigate impacts of the leaf temperature calculation scheme on the carbon assimilation simulation. We find no significant differences in any of the simulated fluxes. For example, the simulated carbon assimilation rate shows only a small difference <0.2 μmol m^{-2} s^{-1} over North-East Asia in July (Fig. 1e–f). Similarly, the differences of the simulated canopy conductance (Fig. 2c, d) and canopy transpiration (Fig. 2g, h) are both negligible. This conclusion is further confirmed by replacing one-common leaf temperature scheme in CoLM_I with the two-leaf temperature scheme. The regionally averaged model results also show that the carbon assimilation rate (Fig. 3), canopy conductance (Fig. 4) and canopy transpiration (Fig. 5) from CoLM_II_2L1T (circle) are nearly indistinguishable from those from CoLM_II (dotted line). Figure 6c, d show the relative difference (%) in the assimilation rate (CoLM_II_2L1T minus CoLM_II) for each PFT, normalized by the results from CoLM_II. Though CoLM_II_2L1T simulates a carbon assimilation that is slightly lower for most PFTs but larger for several PFTs, such as C3 grass and Crop1, the absolute values of such differences are under 2–4% compared to those simulated by CoLM_II.

This minor impact of two-leaf temperatures on the carbon assimilation results from two factors: (a) the temperature dependence of the assimilation is not that strong, less than a 10% change for a 1 K temperature change (as inferred from Eq. 4a of Table 1); (b) substantial

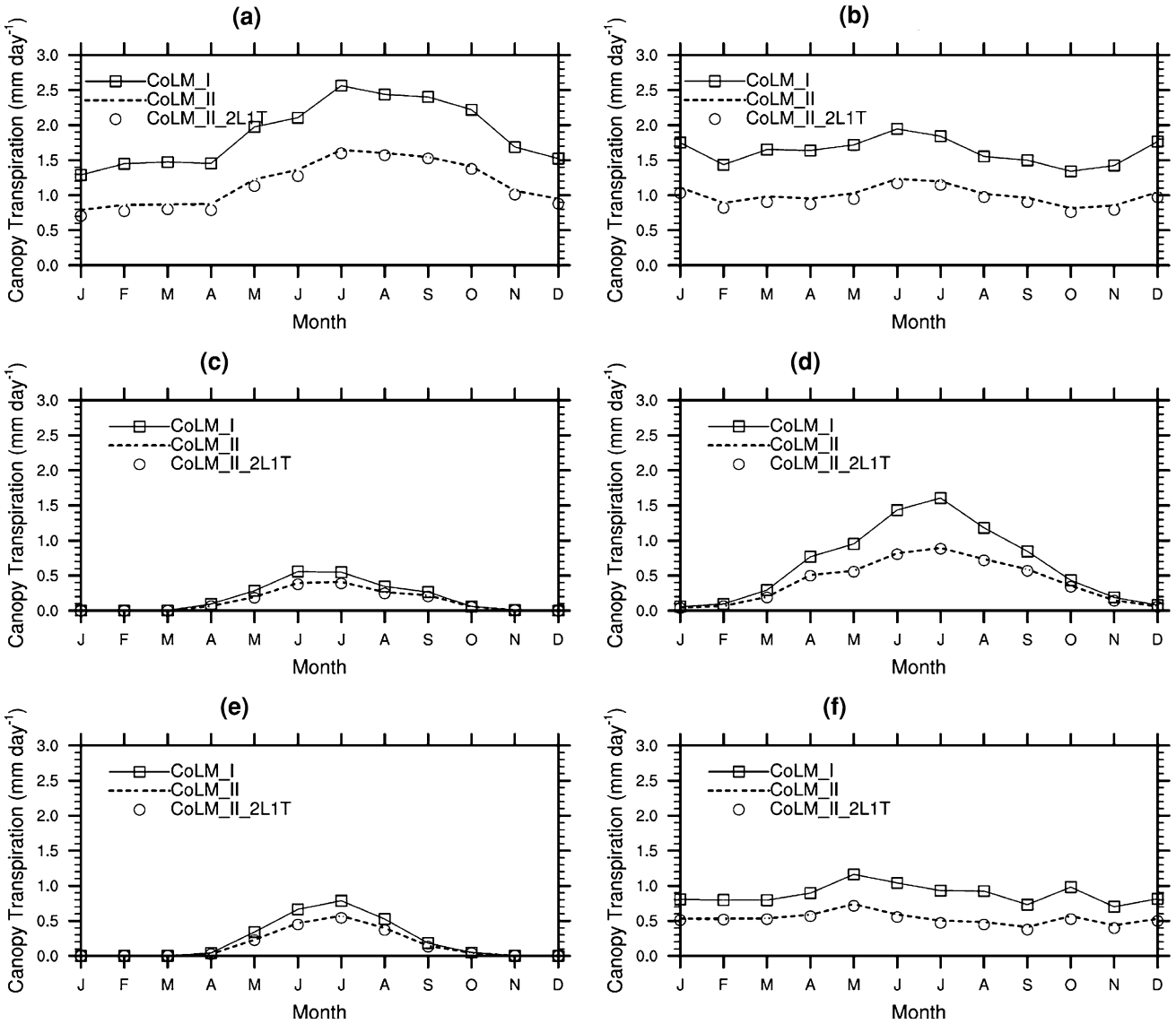

Fig. 5 As in Fig. 3, but for canopy transpiration. **a** Amazon Basin, **b** Congo Basin, **c** Northern North America, **d** South–East North America, **e** Northern Eurasian, **f** South–East Asia

cancellation occurs because of the near linear dependence of the assimilation on leaf temperature and of the leaf temperature variation on incident radiation. In other words, the area weighted average leaf temperature in Scheme II is about the same as the leaf temperature in Scheme I, and the increase of assimilation for the sunlit leaves in Scheme II is about the same as its decrease for the shaded leaves relative to Scheme I, with weighting by their relative leaf areas. Figure 7 quantifies the differences in the monthly average leaf temperature for each PFT. The two-leaf scheme does give a significant difference in leaf temperature between the sunlit and shaded leaves, producing higher sunlit leaf temperature and lower shaded leaf temperature than the one-leaf scheme. However, the difference between the area weighted average leaf temperature of the two-leaf temperature scheme and the leaf temperature of one common leaf temperature scheme are negligible (blue dots in Fig. 7).

4.3 Smoothing, scaling and residual effects

The above results indicate that the impacts of separate treatment of sunlit versus shaded leaf temperature have a negligible impact. Further investigations are performed below to interpret the differences in the model results in terms of the differences in other three main contributors, i.e., the leaf-to-canopy scaling scheme, the co-limitation methods used to estimate the carbon assimilation rate from three assimilation limiting rates, and parameters of the carbon assimilation sub-model. Because both the canopy

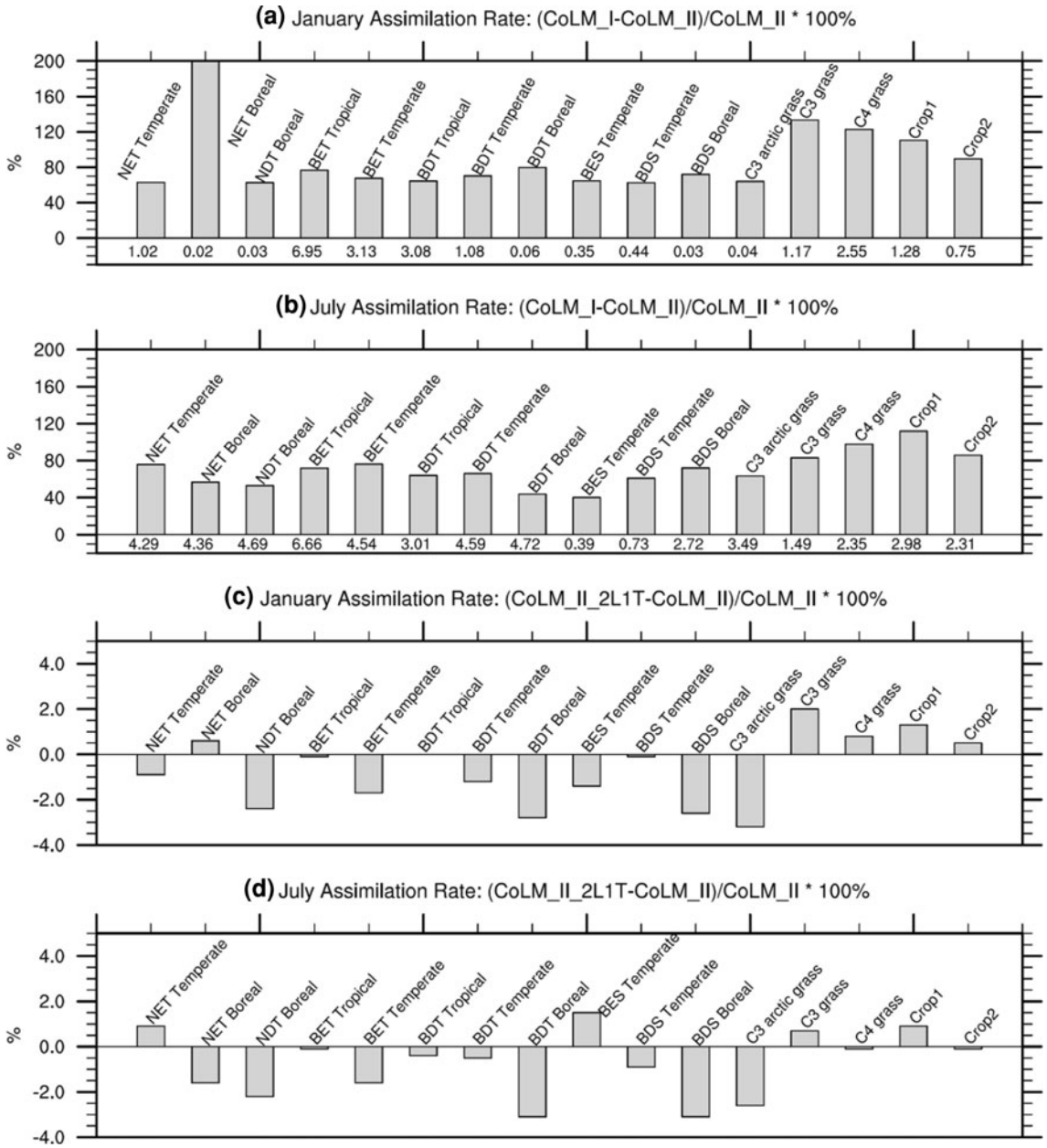

Fig. 6 Carbon assimilation rates for different PFTs simulated by different $A - g_s$ schemes. **a** and **b** differences in percentage (Exp. CoLM_I minus CoLM_II divided by CoLM_II), **c** and **d** differences in percentage (CoLM_II_2L1T minus CoLM_II divided by CoLM_II). The values below the *x*-axis in **a** and **b** represent monthly average assimilation rates (μmol m^{-2} s^{-1}) for each PFT simulated by Exp. CoLM_II

conductance and transpiration strongly depend on the carbon assimilation, only the latter flux was investigated here.

For brevity, most of our analyses were only focused on four sampled PFTs, i.e., tropical broadleaf evergreen tree (BET-Tropical) in Amazon basin (7°S, 67°W), boreal needle leaf evergreen tree (NET-Boreal) in North America (55°N, 125°W), C4 Grass in the subtropics of South America (31°S, 57°W), and temperate broadleaf deciduous shrub (BDS-Temperate) in Australia (31°S, 125°E). The diurnal variations of the assimilation rates for four selected PFTs from different sensitivity experiments are shown in Fig. 8. Table 4 lists the monthly assimilation rates and their difference simulated by different testing schemes, which help to quantify the relative contributions of the different treatments used in the two $A - g_s$ schemes.

Table 4 indicates that much of the difference between CoLM_I and CoLM_II occurs from the assumptions about the scaling and smoothing with the former having the larger effect. Table 4 and Fig. 8 show that after removing both the "smoothing" and "scaling" methods

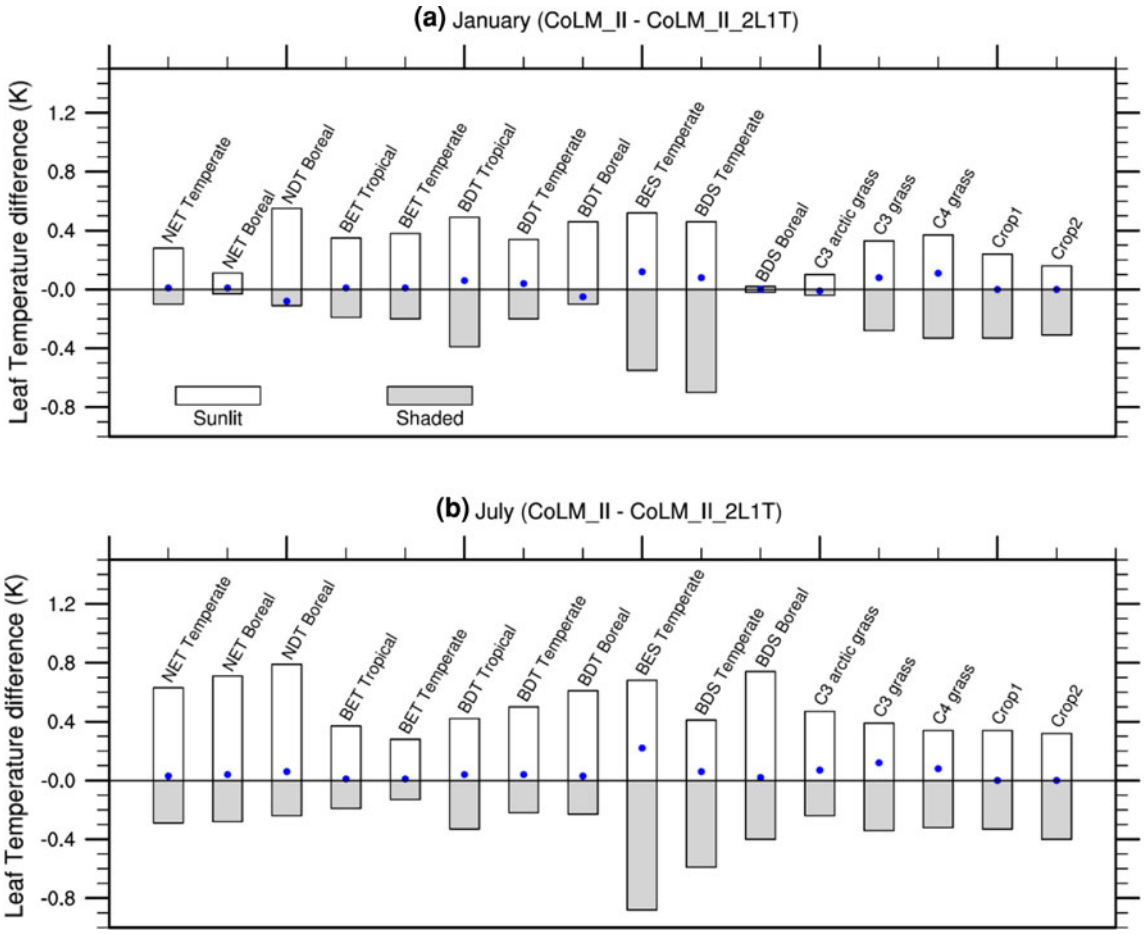

Fig. 7 Leaf temperatures for different PFTs simulated by Exp. CoLM_II and CoLM_II_2L1T. **a** January and **b** July, in which leaf temperatures for sunlit and shaded leaves from CoLM_II_2L1T are compared to the only one leaf temperature calculated by CoLM_II. The *blue dots* represent the area weighted average leaf temperature from the sunlit and shaded leaf temperature

(CoLM_II_sm_scale), the difference between CoLM_I and CoLM_II is much smaller. The scaling and smoothing effects contribute to about 70–80% of the differences between CoLM_I and CoLM_II except for the NET-Boreal, BDS Temperate and C4 Grass in January when photosynthesis is small. Different treatments for the parameters of the carbon assimilation sub-model, i.e., the temperature dependence of V_{max} and Γ_*, cause these relatively small residual effects. Compared to the scaling and smoothing effects, the residual effects are smaller except for January C4 Grass.

In order to evaluate respective impacts of the scaling and smoothing methods, further investigation are also performed on these effects as described below.

4.3.1 Scaling effects

Scheme I calculates the total carbon assimilation rate using an "average" scheme, in which the total assimilation rate is estimated from the assimilation rates of the sunlit leaves and shaded leaves per unit LAI multiplied by weight factors L_{sun} and L_{sha}. However, Scheme II aggregates separately the assimilation rate from leaves to sunlit and shaded fractions of the canopy through integrating the photosynthetic parameters by using scaling factors C_{1sun},C_{1sha},C_{2sun} and C_{2sha} (Eqs. 19–20 and 24–25). After replacing the "scaling" scheme of Scheme II with the "average" scheme (CoLM_II$_{_scale}$), the simulated assimilation rate (dashed line) increases (Fig. 8). Except for July C4 Grass case, the increase of the assimilation rates produced by CoLM_II$_{_scale}$ is evidently larger than that of CoLM_II$_{_sm}$ (square). Compared to the original scheme II (CoLM_II), the simulated assimilation rate of BET-Tropical, NET-Boreal, BDS-Temperate and C4-grass increases by about 39, 62, 70 and 20%, respectively upon the removal of the "scaling" method (Table 4). On average, the simulated assimilation rate from CoLM_II$_{_scale}$ increases by about 40–45% compared to the original scheme II (CoLM_II). However, some exceptions are found in the C4 Grass case, in which the different treatments for the parameters of the

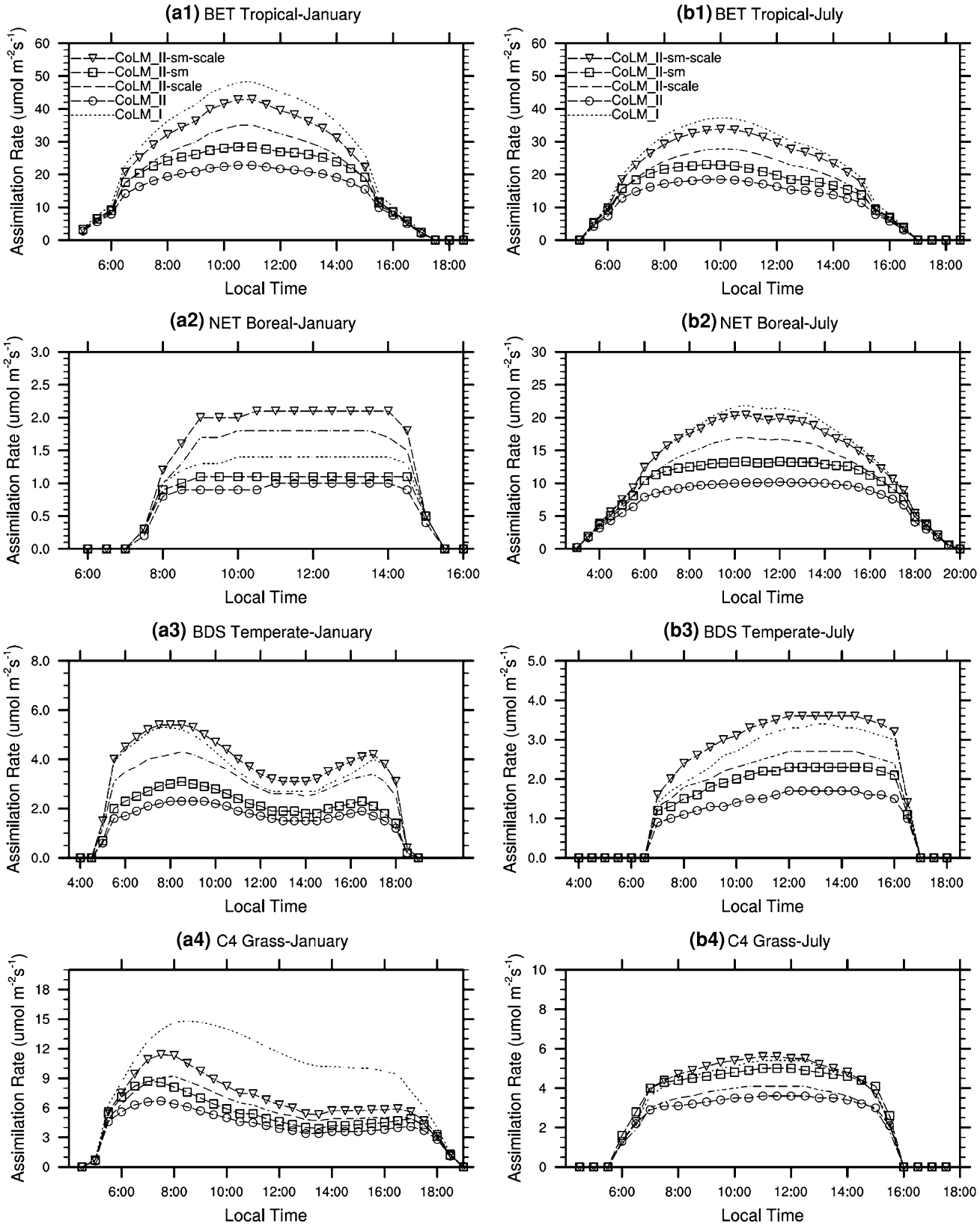

Fig. 8 Averaged diurnal cycle of carbon assimilation rates in μmol m^{-2} s^{-2}(only daytime) for four selected PFTs simulated by $A - g_s$ Scheme I and Scheme II as well as different testing schemes of Scheme II. The description of the legend is the same as in Table 3

Table 4 Differences of monthly assimilation rates (μmol m^{-2} s^{-1}) for BET Tropical, NET Boreal, BDS Temperate and C4 Grass simulated by Scheme I and Scheme II, as well as different tests for Scheme II

CASE	PFT							
	BET Tropical		NET Boreal		BDS Temperate		C4 Grass	
	January	July	January	July	January	July	January	July
CoLM_I	15.73	12.57	0.41	9.78	2.07	1.15	5.97	1.81
CoLM_II	8.32	6.80	0.28	5.34	0.99	0.60	2.52	1.31
CoLM_I-CoLM_II	7.41	5.77	0.13	4.44	1.08	0.55	3.45	0.50
CoLM_II_sm_scale-CoLM_II	5.51	4.74	0.3	3.96	1.26	0.67	1.41	0.58
CoLM_II_scale-CoLM_II	3.18	2.72	0.22	2.50	0.81	0.35	0.81	0.11
CoLM_II_sm-CoLM_II	1.97	1.53	0.06	1.54	0.26	0.23	0.52	0.48
CoLM_I-CoLM_II_sm_scale	1.90	1.03	−0.17	0.48	−0.18	−0.12	2.04	−0.08

carbon assimilation sub-model rather than the scaling approach have the most important impact.

The "scaling" factors involved in the two schemes are directly compared to provide further explanations for the differences in model results due to different scaling schemes. We noted that the co-limitation of the electron transport rate used in Scheme II has very limited impacts on the model results, and so do the corresponding scaling factors C_{2sun} and C_{2sha}. However, the scaling factor C_{1sun} and C_{1sha} plays a major role in producing the difference in the scaling schemes. Essentially, L_{sun} and L_{sha} used in Scheme I are equivalent to the scaling factors C_{1sun} and C_{1sha} (Eqs. 19–20) of Scheme II. Figure 9 shows the scaling factors normalized by L_{sun} and L_{sha} used in Scheme II. The ratios of C_{1sun}/L_{sun} and C_{1sha}/L_{sha} are evidently <1.0 in all cases, and larger L_{sun} and L_{sha} are responsible for the larger carbon assimilation rates given by Scheme I. The difference in the estimated assimilation rate caused by the scaling scheme is mainly attributed to the difference between $C_{1sun}(C_{1sha})$ and $L_{sun}(L_{sha})$. In addition, the seasonality of both C_{1sha} and C_{1sun}, as well as the sensitivity of the parameter estimations in assimilation sub-models to seasonally varying climate factors, are the main reasons for the seasonal difference between the model results discussed.

4.3.2 Smoothing effects

Scheme I estimates the assimilation rate from the minimum of those three limiting factors (the "minimum" method), but Scheme II calculates the assimilation rate by solving two quadratic equations (the "smoothing" method). To examine the impact of the "smoothing" method used by Scheme II, the assimilation rate was recalculated by replacing the "smoothing" method with the "minimum" method as used in Scheme I (CoLM_II$_{sm}$). The diurnal variations of the assimilation rate simulated by CoLM_II$_{sm}$ as well as the original scheme II (CoLM_II) are shown in Fig. 8. The assimilation rate A calculated by CoLM_II (circle) is evidently lower than that calculated by CoLM_II$_{sm}$ (square). In all cases, the assimilation rates are much larger without the "smoothing" method. Compared to the original Scheme II, the monthly average A increases by about 23, 25, 27 and 24% for BET-Tropical, NET-Boreal, BDS-Temperate and C4-grass, respectively (Table 4). The monthly average A increases by about 25% on average after removing the "smoothing" method. Evidently, the "smoothing" method of Scheme II lowers the value of A significantly compared to the "minimum" method of Scheme I.

In summary, the different treatments in three aspects are mainly responsible for the difference in the carbon assimilation simulations between CoLM_I and CoLM_II, and the leaf-to-canopy scaling approach is the largest contributor to the simulation discrepancies. The two-leaf temperature scheme produces distinctly different sunlit and shaded leaf temperatures but has little impacts on the simulation of carbon assimilation. It is not the differences in leaf temperature but rather the amount of leaves illuminated and their photosynthetic capacity that matter. The different methods of co-limitation of assimilation rate show secondary impacts on the results. Except for a few biomes, the residual effects caused by the different methods used to estimate assimilation rate and the different parameter estimations in the carbon assimilation sub-models have smaller impacts on the simulated values of carbon assimilation. It is also noted that different responses induced by PFT-dependent phenological and physiological parameters exist among the sampled PFTs.

5 Conclusion

In this paper, we compared the carbon assimilation rate, canopy conductance and canopy transpiration simulated by two carbon assimilation and stomatal conductance ($A - g_s$) schemes, a relatively simple $A - g_s$ scheme with

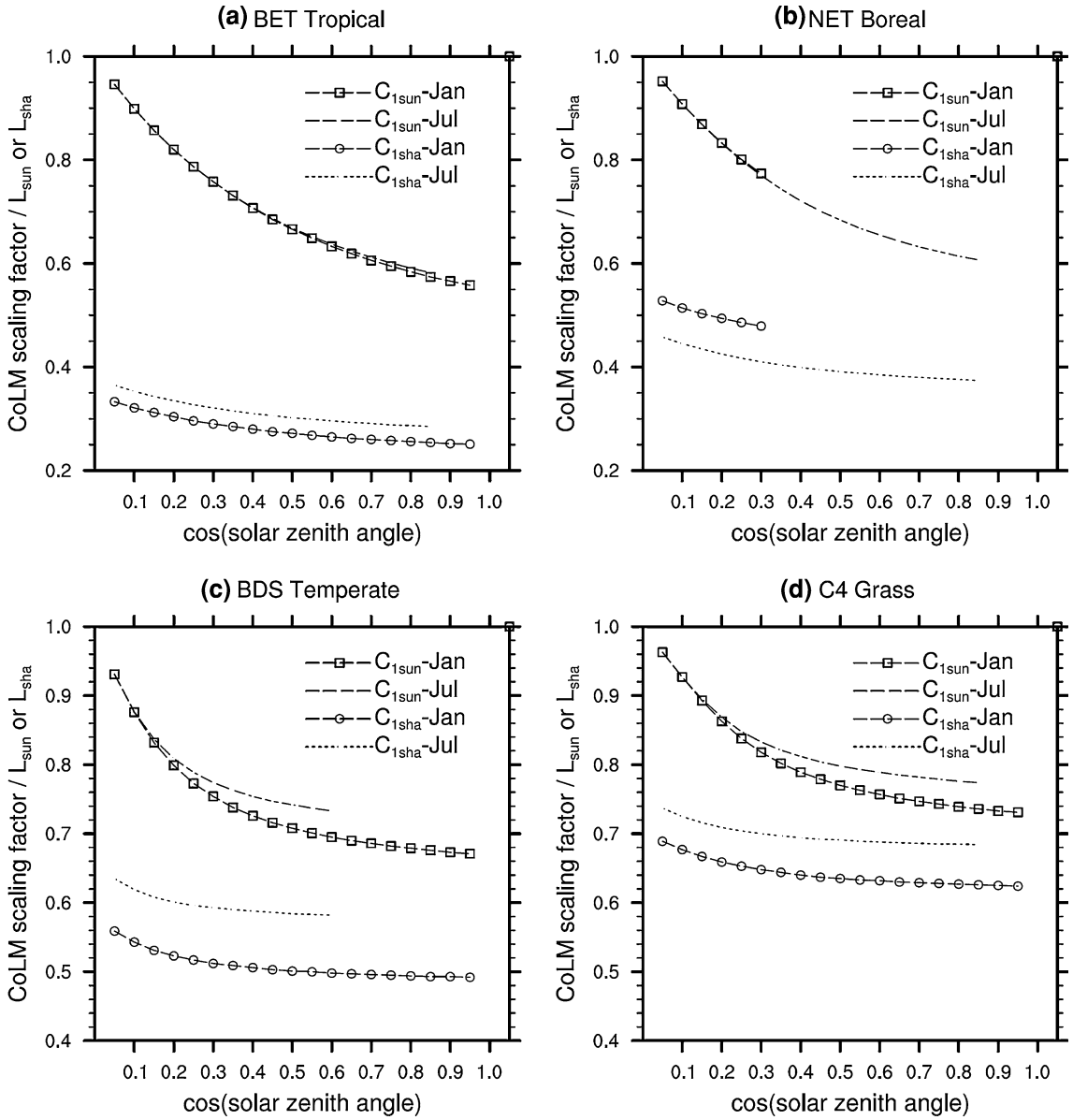

Fig. 9 Scaling factors used by $A - g_s$ Scheme II for sampled PFTs. **a** BET Tropical ($L_{AI} = 5.4$ and 4.8 January and July, respectively), **b** NET Boreal ($L_{AI} = 2.75$ for January and 3.5 for July), **c** BDS Temperate ($L_{AI} = 2.4$ and 1.8 January and July, respectively), **d** C3 Grass ($L_{AI} = 0.6$ for January and 0.9 for July)

parameterizations from the NCAR model (Scheme I) and a two-big leaf $A - g_s$ scheme newly developed by Dai et al. (2004) (Scheme II), to quantify the impacts of different treatments of canopy stomatal conductance and carbon assimilation on the estimations of carbon assimilation and canopy transpiration.

Scheme I was found to differ from Scheme II substantially in its simulated carbon assimilation rate and canopy transpiration. It gives larger estimates for carbon assimilation rate, canopy conductance and canopy transpiration than Scheme II, Its estimates of carbon assimilation are larger by over 60–75% for most PFTs and even above 100% for C3 grass, C4 grass and crop1. Such different model estimates can be attributed to:

1. Different leaf-to-canopy scaling schemes: the "average" scheme used in Scheme I produces a larger carbon assimilation rate than the "scaling" scheme of Scheme II;
2. Co-limitation methods used to estimate carbon assimilation rate from assimilation limiting rates: the "minimum" method of Scheme I gives a larger value than the "smooth" method of Scheme II;
3. Residual effects induced by differences in the carbon assimilation sub-models: Scheme I produces a larger

carbon assimilation rate than Scheme II in most cases and a slightly smaller value for a few biomes.

The leaf-to-canopy scaling method makes a major contribution to the different model results. Introducing co-limitation has a lesser but still important effect. Except for a few biomes, the residual effects due to other parameterization differences have relatively small impacts on the simulated values of carbon assimilation. The two-leaf temperature scheme produces distinctly different sunlit and shaded leaf temperatures but has little impacts on the simulation of carbon assimilation.

Our model-based sensitivity experiments indicate that differences in $A - g_s$ schemes can produce large differences in the estimate of terrestrial carbon assimilation and canopy transpiration. By identifying major factors and their relative roles in contributing to the resulting model differences, this study provides some very useful information to improve land surface model parameterizations in the estimation of carbon assimilation and canopy transpiration. Models can differ in both their structure and parameters. In this study, parameters have been kept fixed to examine the consequences of structural differences. However, the impacts of structural differences could to a large extent be compensated by parameter adjustment. In particular, assimilation and transpiration are nearly proportional to V_{cmax}. Scheme I could have fixed V_{max} to a lower constant value to compensate for its decrease within the canopy and the lack of smoothing in matching the different limiting rates. More generally, simplified models are only likely to reproduce canopy level observations, if constrained by them, when parameter values specified at leaf level recognize within canopy differences.

Previous studies found that the photosynthetic parameters are important sources of uncertainty in the simulation of the vegetation dynamics (Hallgren and Pitman 2000). A large range has also been found in some photosynthetic parameters between species (even among the same species) as estimated from the gas exchange measurements (Wullscheger 1993). Fortunately, FLUXNET provides extensive canopy level data to study the temporal and spatial variability of ecosystem-scale carbon dioxide, water vapor, and energy fluxes (Baldocchi et al. 2001). After such field observations are used to optimize model parameters, further numerical experimentation would be appropriate to identify the consequences of different model parameterizations. Once the parameter values are properly chosen higher order statistics than the climatological means considered here may be needed to evaluate different treatments used in $A - g_s$ schemes and guide the best choice of a scheme.

Acknowledgments Haishan Chen has been supported by NSF of China (NSFC) under Grant 40875057, 40405018 and the Special Funds for Public Welfare of China (Grant No. GYHY(QX) 2007-6-25). Yongjiu Dai acknowledges support from NSF of China (NSFC) under Grant 40775041. R. Dickinson has been supported by the US NSF grant ATM-0921898 and DOE grant DE-F602-01ERG3198. We acknowledge use of the GSWP-2 near surface meteorology dataset. We also thank Qing Liu, Yuhong Tian and Junfeng Miao for insightful discussions and helpful comments.

References

Baldocchi DD, Harley PC (1995) Scaling carbon dioxide and water vapor exchange from leaf to canopy in a deciduous forest II: model testing and application. Plant Cell Environ 18:1157–1173

Baldocchi D, Falge E, Gu L, Olson R, Hollinger D, Running S, Anthoni P, Bernhofer C, Davis K, Evans R, Fuentes J, Goldstein A, Katul G, Law B, Lee X, Malhi Y, Meyers T, Munger W, Oechel W, Paw KT, Pilegaard K, Schmid HP, Valentini R, Verma S, Vesala T, Wilson K, Wofsy S (2001) FLUXNET: a new tool to study the temporal and spatial variability of ecosystem-scale carbon dioxide, water vapor, and energy flux densities. Bull Am Meteor Soc 82:2415–2434

Ball JT (1988) An analysis of stomatal conductance. Ph.D. thesis, Stanford University, 89 pp

Ball JT, Woodrow IE, Berry JA (1987) A model predicting stomatal conductance and its contribution to the control of photosynthesis under different environmental conditions. In: Biggens J (ed) Progress in photosynthesis research. Martinus-Nijhoff Publishers, Dordrecht, pp 221–224

Bonan GB (1996) A land surface model (LSM version 1.0) for ecological, hydrological, and atmospheric studies: technical description and user's guide. Technical report NCAR technical note—417+ STR, NCAR, Boulder, CO 80307, USA

Bonan GB (1998) The land surface climatology of the NCAR land surface model coupled to the NCAR community climate model. J Clim 11:1307–1326

Bonan GB, Oleson KW, Vertenstein M, Levis S, Zeng X, Dai Y, Dickinson RE, Yang Z-L (2002) The land surface climatology of the community land model coupled to the NCAR community climate model. J Clim 15:3123–3149

Collatz GJ, Berry JA, Farquhar GD, Pierce J (1990) The relationship between the Rubisco reaction mechanism and models of leaf photosynthesis. Plant Cell Environ 13:219–225

Collatz GJ, Ball JT, Grivet C, Berry JA (1991) Physiological and environmental regulation of stomatal conductance, photosynthesis, and transpiration: a model that includes a laminar boundary layer. Agricult Forest Meteorl 54:107–136

Collatz GJ, Ribas-Carbo M, Berry JA (1992) Coupled photosynthesis-stomatal conductance model for leaves of C4 plants. Aust J Plant Physiol 19:519–538

Dai Y (2005) The common land model (CoLM) user's guide. Available via DIALOG. http://climate.eas.gatech.edu/dai/CLM_userguide.doc

Dai Y, Zeng Q-C (1997) A land surface model (IAP94) for climate studies, part I: formulation and validation in off-line experiments. Adv Atmos Sci 14:433–460

Dai Y, Zeng X, Dickinson RE et al (2001) Common land model: technical documentation and user's guide. Available via DIALOG. http://climate.eas.gatech.edu/dai/clmdoc.pdf

Dai Y, Zeng X, Dickinson RE, Baker I, Bonan G, Bosilovich MG, Denning A, Dirmeyer PA, Houser PR, Niu G, Oleson KW, Schlosser CA, Yang Z (2003) The common land model (CLM). Bull Am Meteorol Soc 84:1013–1023

Dai Y, Dickinson RE, Wang Y-P (2004) A two-big-leaf model for canopy temperature, photosynthesis and stomatal conductance. J Clim 17:2281–2299

Dang QL, Margolis HA, Coyea MR, Sy M, Collatz GJ (1997) Evidence concerning the effects of water potential and vapor pressure difference on branch-level gas exchange of boreal tree species in northern Manitoba. Tree Physiol 17:521–536

de Pury DGG, Farquhar GD (1997) Simple scaling of photosynthesis from leaves to canopy without the errors of big leaf models. Plant Cell Environ 20:537–557

Dickinson RE, Henderson-Sellers A, Kennedy PJ, Wilson MF (1986) Biosphere–atmosphere transfer scheme (BATS) for the NCAR community climate model. Technical report NCAR technical note—275+ STR, NCAR, Boulder, CO 80307, USA

Dickinson RE, Henderson-Sellers A, Kennedy OJ (1993) Biosphere atmosphere transfer scheme (BATS) version le as coupled to the NCAR community climate model. Technical report NCAR technical note—387+ STR, NCAR, Boulder, CO 80307, USA

Dickinson RE, Shaikh M, Bryant R, Graumlich L (1998) Interactive canopies for a climate model. J Clim 11:2823–2836

Dickinson RE, Oleson KW, Bonan G, Hoffman F, Thornton P, Vertenstein M, Yang Z-L, Zeng X (2006) The community land model and its climate statistics as a component of the community climate system model. J Clim 19:2302–2324

Farquhar GD, von Caemmerer S, Berry JA (1980) A biochemical model of photosynthetic CO_2 assimilation in leaves of C species. Planta 149:78–90

Field C (1983) Allocating leaf nitrogen for the maximization of carbon gain: leaf age as a control on the allocation program. Oecology 56:341–347

Hallgren WS, Pitman AJ (2000) The uncertainty in simulations by a global biome model (BIOME3) to alternative parameter values. Glob Change Biol 6:483–495

Harley P, Baldocchi DD (1995) Scaling carbon dioxide and water vapor exchange from leaf to canopy in a deciduous forest: I. leaf model parameterization. Plant Cell Environ 18:1146–1156

Harley PC, Thomas RB, Reynolds JF, Strain BR (1992) Modelling photosynthesis of cotton grown in elevated CO_2. Plant Cell Environ 15:271–282

Hirose T, Werger MJA (1987) Maximising daily canopy photosynthesis with respect to the leaf nitrogen allocation pattern in the canopy. Oecology 72:520–526

Jarvis PG (1976) The interpretation of the variations in leaf water potential and stomatal conductance found in canopies in the field. Philos Trans R Soc Lond 273(B):593–610

Jarvis PG (1993) Prospects for bottom-up models. In: Ehleringer JR, Field CB (eds) Scaling physiological processes: leaf to globe. Academic Press, New York, pp 115–126

Jarvis PG (1995) Scaling processes and problems. Plant Cell Environ 18:1079–1089

Kull O, Jarvis PG (1995) The role of nitrogen in a simple scheme to scale up photosynthesis from leaf to canopy. Plant Cell Environ 18:1174–1182

Kull O, Kruijt B (1998) Leaf photosynthetic light response: a mechanistic model for scaling photosynthesis to leaves and canopies. Funct Ecol 12:767–777

Larocque GR (2002) Coupling a detailed photosynthetic model with foliage distribution and light attenuation functions to compute daily gross photosynthesis in sugar maple (*Acer Saccharum Marsh*) stands. Ecol Model 148:213–232

Leuning R (1990) Modeling stomatal behavior and photosynthesis of *Eucalyptus grandis*. Aust J Plant Physiol 17:159–175

Leuning R (1995) A critical appraisal of a combined stomatal photosynthesis model for C3 plants. Plant Cell Environ 18:339–357

Leuning R, Cromer RN, Rance S (1991) Spatial distribution of foliar nitrogen and phosphorus in crowns of *Eucalyptus grandis*. Oecology 88:504–510

Leuning R, Kelliher FM, Depury DGG, Schulze ED (1995) Leaf nitrogen, photosynthesis, conductance and transpiration: scaling from leaves to canopies. Plant Cell Environ 18:1183–1200

Norman JM (1993) Scaling processes between leaf and canopy levels. In: Ehleringer JR, Field CB (eds) Scaling physiological processes: leaf to globe. Academic Press, New York, pp 43–75

Oleson KW, Dai Y, Bonan G, Bosilovich M, Dickinson RE, Dirmeyer P, Hoffman F, Houser P, Levis S, Niu G, Thornton P, Vertenstein M, Yang Z-L, Zeng X (2004) Technical description of the community land model (CLM). Technical report NCAR technical note—461+ STR, NCAR, Boulder, CO 80307, USA

Sellers PJ, Mintz Y, Sud YC, Dalcher A (1986) A simple biosphere model (SIB) for use within general-circulation models. J Atmos Sci 43:505–531

Sellers PJ, Berry JA, Collatz GJ, Field CB, Hall FG (1992) Canopy reflectance, photosynthesis, and transpiration 3: a reanalysis using improved leaf models and a new canopy integration scheme. Remote Sens Environ 42:187–216

Sellers PJ, Randall DA, Collatz GJ, Berry JA, Field CB, Dazlich DA, Zhang C, Collelo GD, Bounoua L (1996) A revised land surface parameterization (SiB2) for atmospheric GCMs 1: model formulation. J Clim 9:676–705

Sellers PJ, Dickinson RE, Randall DA, Betts AK, Hall FG, Berry JA, Collatz GJ, Denning AS, Mooney HA, Nobre CA, Sato N, Field CB, Henderson-Sellers A (1997) Modeling the exchanges of energy, water, and carbon between continents and the atmosphere. Science 275:502–509

Sinclair TR, Murphy CE, Knoerr KR (1976) Development and evaluation of simplified models for simulating canopy photosynthesis and transpiration. J Appl Ecol 13:813–829

Spitters CJT (1986) Separating the diffuse and direct component of global radiation and its implications for modelling canopy photosynthesis Part II: calculation of canopy photosynthesis. Agric Forest Meteorl 38:231–242

Tian Y, Dickinson RE, Zhou L, Shaikh M (2004a) Impact of new land boundary conditions from moderate resolution imaging spectroradiometer (MODIS) data on the climatology of land surface variables. J Geophys Res 109. doi:10.1029/2003JD004499

Tian Y, Dickinson RE, Zhou L, Zeng X, Dai Y, Myneni RB, Knyazikhin Y, Zhang X, Friedl M, Yu H, Wu W, Shaikh M (2004b) Comparison of seasonal and spatial variations of leaf area index and fraction of absorbed photosynthetically active radiation from moderate resolution imaging spectroradiometer (MODIS) and common land model. J Geophys Res 109. doi: 10.1029/2003JD003777

Walcroft AS, Whitehead D, Silvester WB, Kelliher FM (1997) The response of photosynthetic model parameters to temperature and nitrogen concentration in *Pinus radiata D*. Don. Plant Cell Environ 20:1338–1348

Wang Y-P, Jarvis PJ (1990) Description and validation of an array model—MAESTRO. Agric Forest Meteorl 51:257–280

Wang Y-P, Leuning R (1998) A two-leaf model for canopy conductance, photosynthesis and portioning of available energy I: model description and comparison with a multi-layered model. Agric Forest Meteorl 91:89–111

Wang Y-P, Polglase PJ (1995) Carbon balance in the tundra, boreal forest and humid tropical forest during climate change: scaling up from leaf physiology and soil carbon dynamics. Plant Cell Environ 18:1226–1244

Wullschleger SD (1993) Biochemical limitations to carbon assimilation in C3 plants—a retrospective analysis of A/ci curves for 109 species. J Exp Bot 44:907–920

Zhao M, Dirmeyer P (2003) Production and analysis of GSWP-2 near-surface meteorology data sets. Technical report COLA technical report—159, COLA, Calverton, MD20705, USA